UPSTREAM ROUGHNESS EFFECTS ON REATTACHED TURBULENT FLOW OVER FORWARD FACING STEP

E.E. Essel[1], S. Mali[1], E.W. Thacher[1] and M.F. Tachie[1]

[1] University of Manitoba, Winnipeg, MB, Canada, R3T 5V6

essele@myumanitoba.ca

Abstract

An experimental study was performed to investigate the effects of Reynolds number based on approach velocity and step height, Re_h and upstream roughness on the flow characteristics of a smooth forward facing step. The rough wall was produced from sand grains of average diameter 1.5 mm and the Re_h ranged from 2010 to 9130 for both smooth and rough wall experiments. The results for the smooth upstream wall showed that the reattachment length, L_r^* increased monotonically with $Re_h \leq 5800$ before it becomes independent of Reynolds number for the $Re_h > 5800$. Wall roughness, on the other hand, decreased the L_r^* by 16 % when Reynolds number increased from 2230 to 4010. Beyond $Re_h = 4010$, the L_r^* was independent of Re_h. The L_r^* of the rough case was 44 % shorter than values of the smooth case for $Re_h > 5800$. Detailed comparison of the results revealed that the mean velocities, Reynolds shear stress and the ejections and sweeps are weakened by upstream roughness, although, the turbulent kinetic energy is enhanced. The Reynolds shear stress showed very large negative values at vicinity of the leading edge of the step which were found to be majorly contributed by the inward and outward interactions.

1 Introduction

Separated and reattached turbulent flows occur in a wide range of engineering applications such as pipe systems, wind turbines and gas turbines. Such flow phenomena usually generate structural vibrations and noise and may also reduce the efficiency and performance of these fluid-thermal systems. In many engineering applications, factors such as manufacturing defects, harsh operating conditions, corrosion, and biomass accumulation over a period of time will cause the wall to become hydraulically rough. Although the effects of wall roughness on zero pressure gradient boundary layers and fully developed internal flows have been studied in great detail, our understanding of wall roughness effects on separated and reattached turbulent flow is incomplete.

Given its practical applications, considerable research efforts have been made in the past to understand the characteristics of separation and reattachment of turbulent boundary layer caused by obstacles. Majority of these studies concentrated on geometry and flow parameters that affect the flow characteristics over a backward facing step, hence the effects of these parameters on flow over forward facing step (FFS), which is the focus of the present study, is not well understood. Figure 1 shows the pertinent features of separated and reattached flow over a smooth FFS and the Cartesian coordinate system employed in the present study. The x-coordinate is aligned with the streamwise direction, while the y-coordinate is aligned with the wall-normal direction; $x = 0$ is at the leading edge of the step and $y = 0$ is on the upstream wall. The upstream boundary layer of mean velocity, U_e and thickness, δ approaches a FFS of height, h. The presence of the step induces adverse pressure gradient which causes the first flow separation to occur upstream of the leading edge of the step and reattaches on the front of the step. The second detachment occurs at the leading edge of the step and reattaches at a distance, L_r, downstream of the leading edge of the step. The maximum height of the second recirculation region is denoted by h_d. The region beyond the reattachment point is referred to as the redevelopment region.

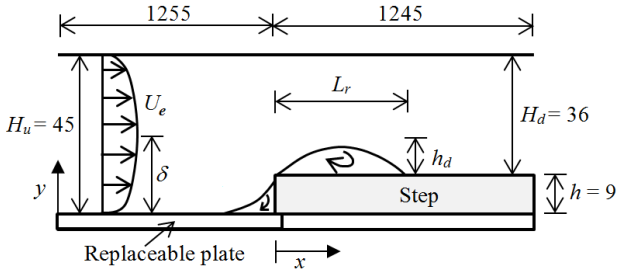

Figure 1: Schematic of FFS test channel. All dimensions in millimetres

The reattachment length, L_r, is found to depend on a variety of parameters such as Reynolds number ($Re_h = U_e h/\nu$, where U_e is the approach mean velocity and ν is kinematic viscosity), ratio of upstream boundary layer thickness to step height (δ/h), blockage ratio ($BR = h/H_u$), aspect ratios (W/h and L/h where W is the channel width and L is the length of FFS), upstream turbulence intensity (Tu) and relative roughness (ε/h). Sherry et al (2010), for example, studied the effects of Re_h ranging from 1400 to 19000

and δ/h (0.83 – 2.5) on the reattachment length. Their step height was varied to give blockage ratios, $0.032 \leq BR \leq 0.097$ and a freestream turbulence level, Tu % = 1.43 % was used in all their experiments. It was found that L_r increased monotonically with Re_h < 8500. Beyond Re_h = 8500, L_r was found to be less sensitive to Reynolds number. Although L_r varied with δ/h, the threshold value of Re_h = 8500 was independent of δ/h.

Most of the previous studies were performed in wind and water tunnels in which the freestream turbulence levels and blockage ratio were fairly low. Furthermore, majority of these studies focussed on smooth upstream wall and smooth FFS. In fact, only the study of Ren and Wu (2011) and its sequel (Wu and Ren (2013)) considered a rough FFS replicated from a realistic turbine blade. In their study, the upstream wall was kept smooth and particle image velocimetry (PIV) was used to conduct measurement at Re_h = 3450 and δ/h = 8. It was found that the mean velocity field on top of the FFS was strongly dependent on the specific roughness topographies.

The present study investigates the effects of effects of wall roughness and Reynolds number on the turbulent transport phenomena in separated and reattached flows on a FFS in a water channel. Detailed PIV measurements were performed at wide Reynolds number range, $2040 \leq Re_h \leq 9130$ over smooth and rough upstream walls against a smooth FFS. The roughness element employed was three-dimensional sand grains because this type of roughness element has been used quite extensively in previous studies of rough wall turbulent boundary layers. Since separated and reattached flows are routinely used as acute test case for numerical models, the knowledge accrued from the present study as well as the benchmark dataset will be critically important for numerical studies on separated and reattached flows.

2 Experimental procedure

The experiments were conducted in a closed test channel that was screwed onto the bottom wall of a main recirculating water channel. As is shown in Figure 1, the test channel was 2500 mm long, 188 mm wide and 45 mm high and was fabricated from clear acrylic plates to facilitate optical access. A smooth step of nominal height, h = 9 mm, 188 mm wide and 1245 mm long was used to induce the flow separation. The step was positioned 1255 mm from the leading edge of the test channel. Smooth and rough upstream walls were investigated by positioning smooth and rough replaceable plates of nominal thickness 6 mm at the upstream of the step, one after another. The smooth replaceable plate was produced from 6 mm thick acrylic plate while the rough replaceable plate was produced from sand grains of average diameter 1.5 mm glued unto a 4.5 mm thick acrylic plate. A Veeco Wyco NT9100 optical profilometer which utilizes white light interferometry with sub-micron vertical accuracy was used to obtain topographical information of the rough wall. The average peak-to-valley roughness height, k = 1.8 mm and the root-mean-square height, k_{rms} = 418 μm. The aspect ratios (W/h = 21 and L/h = 138) of the test section ensured that the flow was nominally two-dimensional at the mid-span (W/h > 10) and the reattachment occurred on top of the step (De Brederode, and Bradshaw (1972) and Largeau and Moriniere (2007)). The blockage ratio was 0.2.

Table 1: Test conditions

Test	U_e (m/s)	Test	U_e (m/s)
S-2040	0.227	R-2230	0.248
S-4030	0.447	R-4010	0.445
S-4940	0.549	R-5100	0.567
S-6380	0.709	R-6480	0.720
S-7090	0.788	R-7000	0.778
S-7740	0.861	R-7450	0.827
S-8360	0.929	R-8150	0.906
S-8750	0.973	R-8700	0.967
S-9130	1.015	R-8950	0.995

For the smooth upstream wall and smooth step, and rough upstream wall and smooth step (hereafter referred to smooth (S) and rough (R), respectively, for brevity), velocity measurements were conducted at 9 different Reynolds numbers. A summary of the upstream test conditions is presented in Table 1 where S-2040, for example, denotes test condition over the smooth upstream wall at Re_h = 2040. Similarly, R-2230 denotes test condition over the rough upstream wall at Re_h = 2230.

Two-dimensional PIV system was used to perform velocity measurements in x-y planes located at the mid-span of the channel. The flow was seeded with 10 μm fluorescent tracer particles, and illuminated with a Nd:YAG double-pulsed laser (120 mJ/pulse). A 12-bit CCD camera fitted with an orange filter was used to image scattered light from the tracer particles. The use of fluorescent particles in conjunction with orange filter for the camera significantly reduced surface glare between the working fluid (water) and the solid wall, hereby improving the quality of the velocity vectors close to the wall. The field of view was set to 5.6 h × 5.6 h in the x and y directions, respectively, and the magnification factor was about 41 pixels/mm. Measurements were performed in an upstream plane centered at -8.0 h to

characterize the upstream boundary layer and in a plane that spans from -2.0 h to 3.5 h to investigate the effects of Reynolds number and upstream roughness on the flow characteristics on top of the step. A sample size of 2000 image pairs were acquired in each measurement plane and post-processed using adaptive correlation method with interrogation area (IA) of 32 pixels × 16 pixels with 50 % overlap. The resulting vector spacing was 0.04 h × 0.02 h in the x and y directions, respectively. During the experiment, precautionary guidelines recommended by Forliti et al (2000) were followed to reduce both bias and precision errors. The uncertainty in the mean velocities at 95 % confidence level was ± 2 % of the streamwise velocity. The uncertainties in the turbulence intensities and Reynolds shear stress are, respectively, estimated to be 7 % and ± 10 % of the peak values.

3 Results and discussion

A. Upstream Boundary Layer: The initial conditions of the approach flow were examined using one-dimensional profiles of the turbulence statistics obtained at $x^* = x/h$ = - 8 over both smooth and rough upstream walls. Figure 2 shows profiles of the streamwise mean velocity (U) at selected Reynolds numbers over both smooth and rough upstream walls. The dashed lines indicate the wall-normal location of the step ($y^* = y/h$ = 1). The corresponding approach mean velocity, U_e shown in Table 1 was used as the velocity scale ($U^* = U/U_e$). For the smooth wall, the mean velocity profiles were less sensitive to Reynolds number. The impact of upstream roughness, however, caused a significant reduction in the flatness of the mean velocity profiles. At y^* = 1, for example, the approach velocity, U^* = 0.870 and 0.734, respectively, over the smooth (S-8750) and rough (R-8700) walls which suggest that the approach velocity reduced by 16 % over the rough compared to the smooth wall. The momentum deficit over the rough wall increased as Reynolds number increased. The

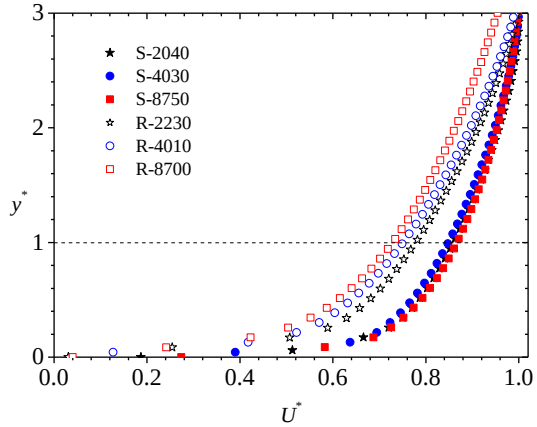

Figure 2: Profiles of upstream streamwise mean velocity at selected Reynolds numbers over smooth (S) and rough (R) walls

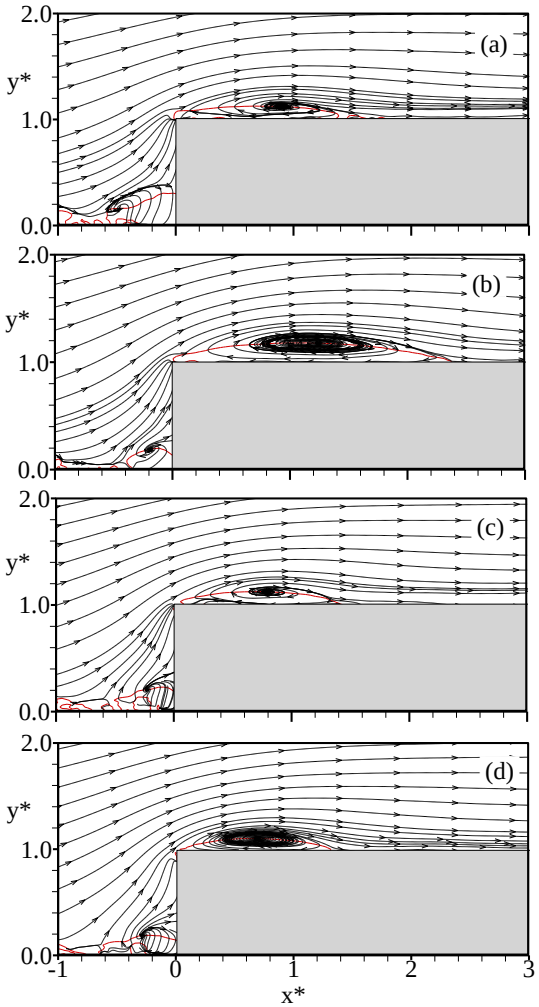

Figure 3:Mean streamlines in the recirculation zones for smooth case at Re_h = 2040 (a) and 8750 (b) and rough wall at Re_h = 2230 (c) and 8700 (d). The contour line represents zero mean velocity.

boundary layer thickness increased monotonically with increasing Reynolds number from δ/h = 2.4 to 2.8 over the smooth wall and δ/h = 2.9 to 3.7 over the rough wall. Although the same roughness elements were used in all the rough wall experiments, the dimensionless equivalent sand grain roughness height increased from k_s^+ = 12 (transitional rough regime) at Re_h = 2230 to k_s^+ > 70 (fully rough regime) for Re_h > 6480. Wall roughness also caused a significant increase in the turbulence level throughout the boundary layer. At the core region of the channel, the turbulence level was about 4% and 5%, respectively, over the smooth and rough walls.

B. Separated and Reattached Region: Mean streamlines at Re_h = 2040 and 8750 for the smooth wall and Re_h = 2230 and 8700 for the rough wall are shown in Figure 3 to examine how the mean flow pattern changes with Re_h and upstream roughness. In each case, distinct recirculation bubbles are observed at the corner of the step and the upstream wall and on top of the step. For the reference smooth case, the physical size of the recirculation bubble on top of the step increased with increasing Re_h. For the rough

case, on the other hand, a decrease in the size of the bubble was observed as Reynolds number increased. To better quantify the effects of Re_h and upstream roughness on the size of the recirculation bubble, the reattachment lengths were evaluated. The reattachment point was estimated as the x-location at which the mean dividing streamline, 50% forward flow fraction, and zero mean velocity from the leading edge of the step intersect with the step. As is seen in Figure 3, the locations at which zero mean velocity and dividing streamline on the step are similar. The differences in reattachment points estimated using the various independent methods was about 0.1 h. The uncertainty of the reattachment length was estimated as ± 0.05 h.

Figure 4a show the variation of L_r^* with Re_h. For the smooth wall, L_r^* initially increased sharply from L_r^* = 1.4 at Re_h = 2040 to L_r^* = 2.2 at Re_h = 4940 but became nearly independent of Reynolds number for Re_h > 5800. A similar variation of L_r^* with Re_h was observed by Sherry et al (2010), although, the threshold Re_h = 5800 in present study is lower than Re_h = 8500 reported in the previous study. The reattachment lengths for the reference smooth wall are approximately 40 % shorter than the previous water tunnel results at comparable δ/h and Re_h values. These differences may be attributed to the relatively high background turbulence level (4.0 %) and blockage ratio (0.20) in the present experiments compared with Tu % = 1.4 % and BR = 0.03 used in Sherry et al (2010). For the rough case, the reattachment length at the lowest Re_h is similar to the smooth wall value. Subsequently, L_r^* decreased to a value of 1.2 at

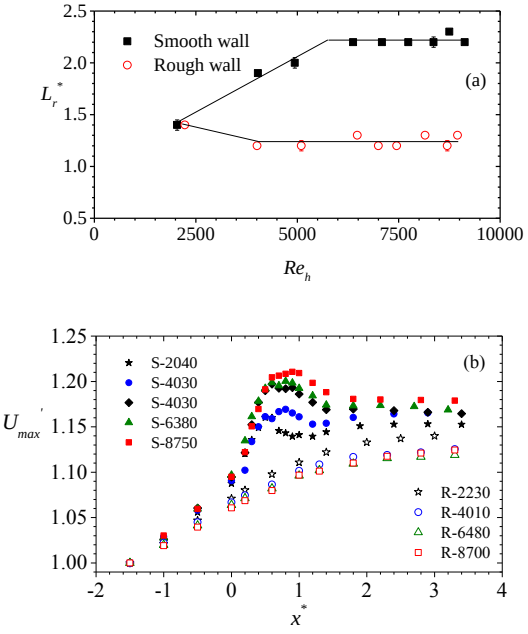

Figure 4: Profile of reattachment length, L_r^* vs Reynolds number, Re_h (a) and distribution of maximum mean velocity, U_{max}^* (b)

Re_h = 4010 and remained independent of Re_h. These results demonstrate that wall roughness significantly decreased the reattachment length which may partly be explained by the concomitant increase in turbulence levels and momentum deficit produced by the upstream roughness. Furthermore, the manner in which L_r^* changes with Re_h is dependent on the wall boundary condition.

Due to the requirement of mass conversation, the mean flow accelerate from the leading edge of the step. To quantify the effects of Re_h and upstream roughness on this process, the distribution of local maximum streamwise mean velocity (U_{max}) normalized by corresponding maximum velocity at x^* = -1.5 is shown in Figure 4b. The scaling employed minimized Re_h effects on U_{max} at the x-locations upstream the step for each wall condition. On top of the step of the smooth upstream wall, U_{max} increased markedly to a local peak value that tends to increase with Re_h. The U_{max} for a given Re_h over the rough wall, on the other hand, increased gradually and monotonically with increasing streamwise distance from the edge of the step. For the rough, note that the distribution is independent of $Re_h \geq 4010$ but these values are about 2 % lower than the values at the lowest Reynolds number (Re_h = 2230).

Figure 5 shows contour plots of the wall-normal mean velocity (V). Very large positive values of V (up to $0.55U_e$ and $0.47U_e$, for the smooth and rough cases, respectively) are observed in the vicinity of the leading edge of the step which should be expected since the fluid is deflected upwards as it approaches the step. Further downstream, regions of negative velocities are observed. These negative velocities may be associated with the entrainment of freestream into the separated shear layer. Such entrainment enhances turbulent mixing and reattachment of the shear layer. The location of the intense negative velocities over

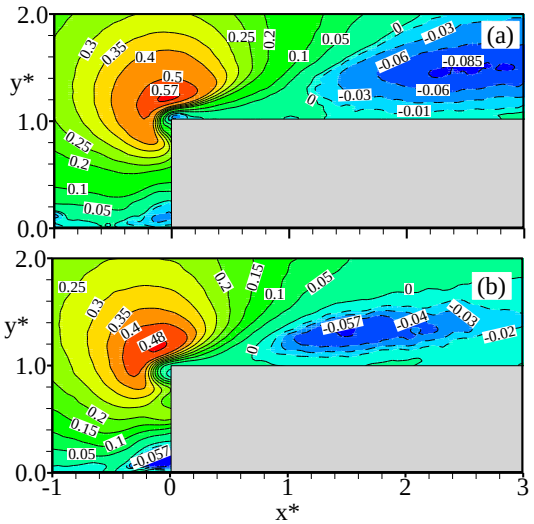

Figure 5: Contour plots of wall-normal mean velocity for smooth case at Re_h = 8750 (a) and rough case at Re_h = 8700 (b)

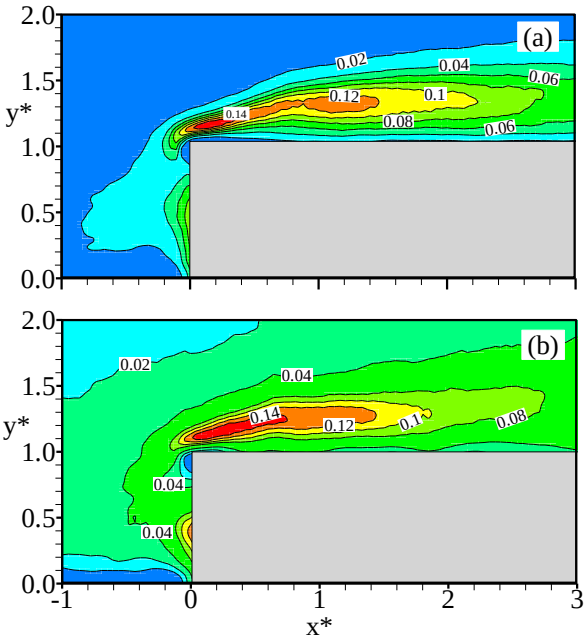

Figure 6: Contour plots of turbulent kinetic energy for smooth case at Re_h = 8750 (a) and rough case at Re_h = 8700 (b)

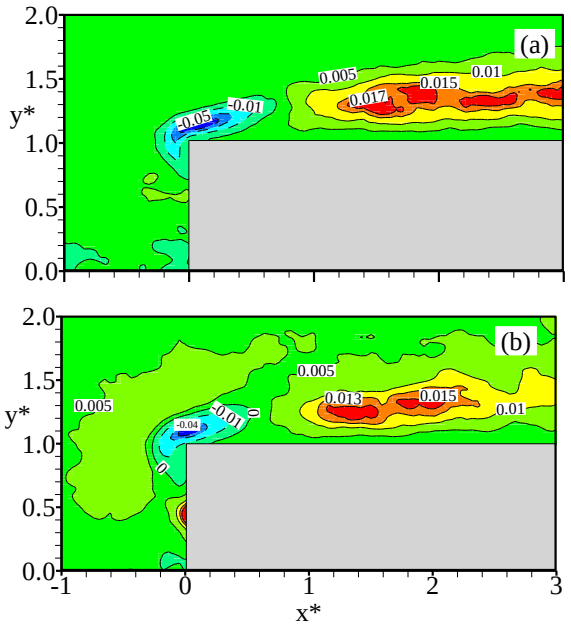

Figure 7: Contour plots of Reynolds shear stress for smooth case at Re_h = 8750 (a) and rough case at Re_h = 8700 (b)

the step is further downstream for the smooth case than the rough case. This should be expected in view of the markedly larger reattachment length for the smooth than the rough case at these Reynolds numbers.

Contour plots of the turbulent kinetic energy (*tke*) and Reynolds shear stress, $<-u'v'>$ are shown in Figure 6 and 7 to examine the turbulence field and investigate the effects of upstream roughness. The *tke* was estimated as 0.70 ($<u'^2> + <v'^2>$) based on the findings of previous studies on separated and reattached flows e.g. Jovic (1996). Irrespectively of upstream condition, the *tke* is significantly enhanced as the approach fluid accelerates pass the leading edge of the step. The enhancement of *tke* may be attributed to the large scale structures that are generated due to separation. Close to the edge of the step, the maximum *tke* is similar for both upstream wall conditions. The values of $<-u'v'>$ are negative close to the leading edge but become positive further downstream on the step. Wall roughness significantly reduced both the negative and positive values of $<-u'v'>$. In Figure 7, for example, upstream roughness reduced the peak value of negative $<-u'v'>$ by about 20 % and the peak value of positive $<-u'v'>$ by about 12 %.

Quadrant decomposition was also used to investigate the dominant Reynolds shear stress contributors. Following the methodology detailed in Lu and Willmarth (1973), the Reynolds shear stress was sort into four different quadrants; outward interaction ($Q1$ events), ejections ($Q2$ events), inward interactions ($Q3$ events) and sweeps ($Q4$ events) using hyperbolic hole, H = 0. The contour plots of the four quadrant events for the rough case at Re_h = 8700 are shown in Figure 8. The corresponding plots for the smooth case were not shown because they are qualitatively similar to the rough case. Close to the leading edge, both $Q1$ and $Q3$ contribute significantly to negative $<-u'v'>$, although the major contributor was $Q3$. The peak value of $Q3$ shown in Figure 8, for example, was 39 % larger than corresponding value of $Q1$. Beyond the leading edge, majority of the $<-u'v'>$ was almost equally contributed by the $Q2$ and $Q4$ events. The $Q1$ and $Q3$ events were independent of roughness, however, $Q2$ and $Q4$ decreased in the case of the upstream rough wall.

Profiles of streamwise mean velocity, turbulent kinetic energy, Reynolds shear stress and triple velocity correlations obtained at selected x-locations in the recirculation region; $x^* = 0$, $0.5L_r^*$, L_r^* and early redevelopment region; $x^* = 1$ of the smooth case (Re_h = 8750) and rough case (Re_h = 8700) are shown in Figure 9 and 10 to quantify the effects of upstream roughness on the flow characteristics. For each wall condition, the streamwise mean velocity profile close to the wall gradually recover from the distortion caused by the severe adverse pressure gradient as streamwise distance increases. The maximum backflow was about $0.17U_e$ and $0.14U_e$ for the smooth and rough wall, respectively. Wall roughness reduced the levels of the streamwise mean velocity in the region away from the wall. As can be observed, the effects of upstream wall roughness increased the peak values of *tke* but decreased the peak values $<-u'v'>$ of the rough case compared to the smooth case. At the leading edge of the step ($x^* = 0$), the large negative peaks of $<-u'v'>$ are noticeable for both test

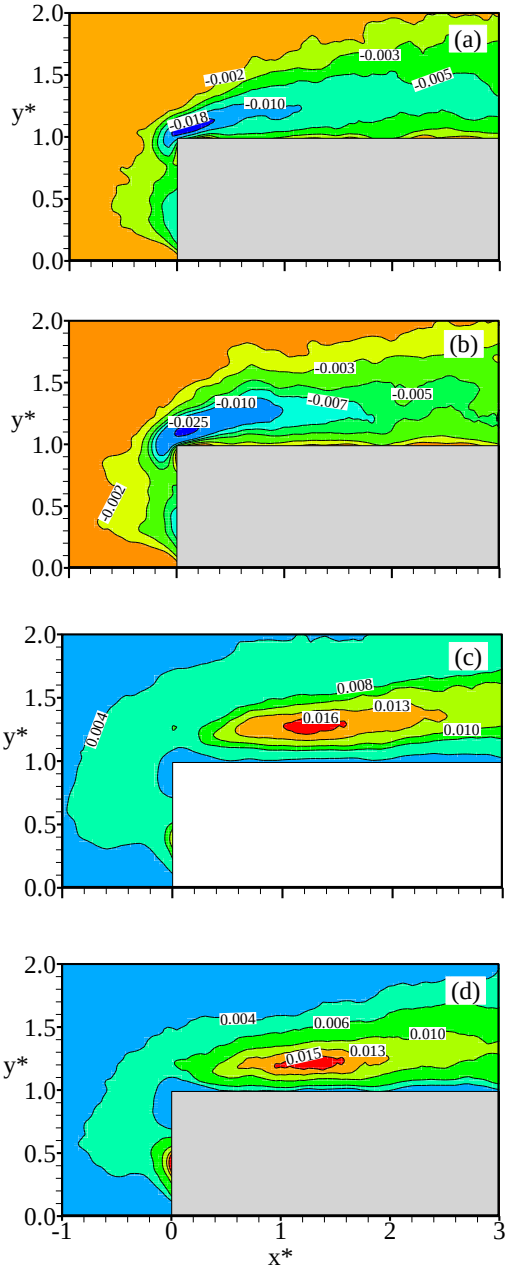

Figure 8: Contour plots of dimensionless Q1(a), Q3 (b), Q2 (c) and Q4 (d) events of hole size, H = 0 for rough case at Re_h = 8700

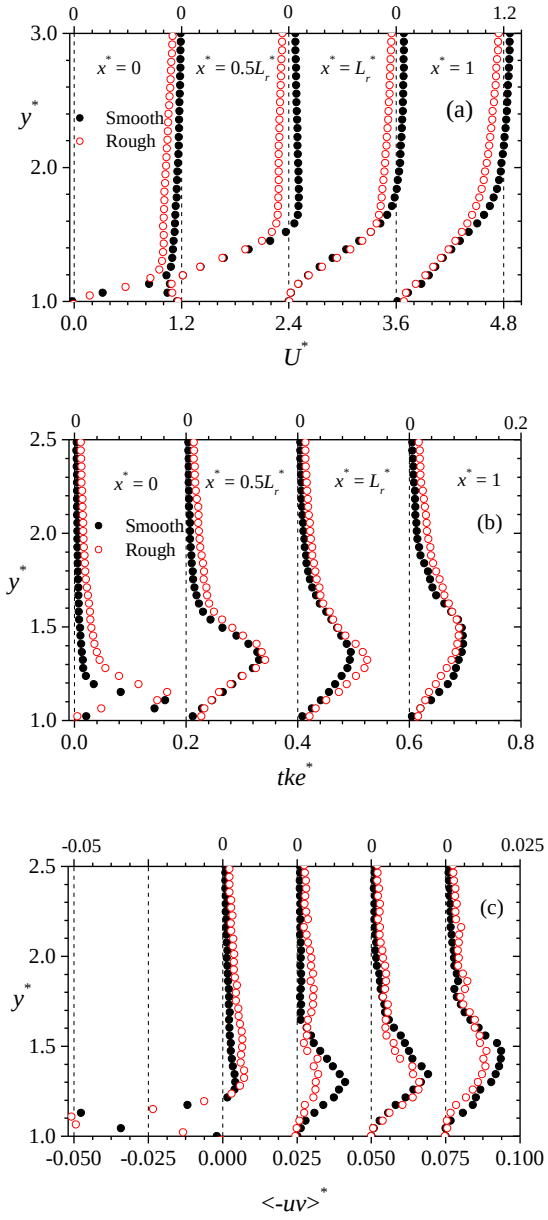

Figure 9: Profiles of streamwise mean velocity (a), turbulent kinetic energy (b) and Reynolds shear stress (c) for smooth case at Re_h = 8750 and rough case at Re_h = 8700

conditions. The maximum $\langle -u'v' \rangle^*$ = 0.019 and 0.016 for smooth and rough cases, respectively. Similar to the Reynolds shear stress, $\langle u'^2 v' \rangle$ and $\langle v'^3 \rangle$ show large negative peaks at x^* = 0 before changing sign further downstream. The effects of upstream roughness on the triple velocity correlations are dependent on the specific streamwise locations. At centre of the recirculation bubble ($x^* = 0.5L_r^*$), for example, wall roughness enhanced the peak values of the profiles of the triple velocity correlations. At reattachment point and early redevelopment region, on the other hand, the peak values of the triple velocity correlations are reduced over the rough case compared to the smooth case.

4 Conclusion

PIV measurements were conducted in *x-y* planes located upstream and downstream of the leading edge of a smooth forward facing step. Two replaceable walls; reference smooth acrylic wall and rough wall produced from sand grains of average diameter 1.5 mm were position upstream of the step, one after another, to investigate the effects of upstream roughness on the separated and reattached flow. For each wall condition, a wide range of Reynolds number ($2040 \leq Re_h \leq 9130$) was investigated. The results

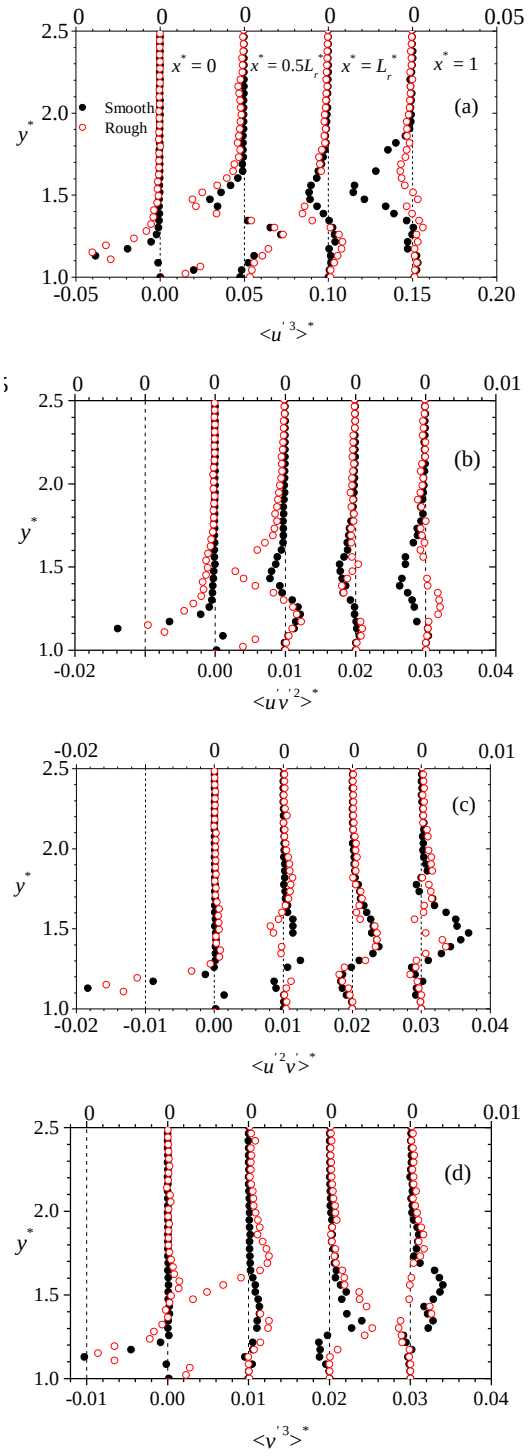

Figure 10: Profiles of triple velocity correlations for smooth case at Re_h = 8750 and rough case at Re_h = 8700

showed that the reattachment length, L_r^*, was independent of Reynolds number for Re_h > 5800 over the smooth wall and Re_h > 4010 over the rough wall. Before the respective threshold Re_h, L_r^* increased monotonically with Re_h for the smooth case but decreased in the case of the rough wall. The impact of roughness reduced the reattachment length, mean velocities and Reynolds shear stress but enhanced the turbulent kinetic energy in the recirculation region and early redevelopment region. Upstream roughness increased the peak values of the triple velocity correlations within the recirculation region but reduced the levels in the early redevelopment region. Quadrant decomposition of the dominant Reynolds shear stress contributors revealed that the inward and outward interactions are dominant at the vicinity of the leading edge of the step and these events are independent of roughness. The effects of upstream roughness, however, decreased the ejections and sweeps.

Acknowledgement

The authors acknowledge the support of this work by the Natural Sciences and Engineering Research Council of Canada and the profiling results of the rough wall by Dr. Karen Flack of United States Naval Academy.

References

Sherry, M., Lo Jacono, D., and Sheridan, J. (2010), An experimental investigation of the recirculation zone formed downstream of a forward facing step, *J. Wind Eng. Ind. Aerodyn.*, Vol. 98(12), pp. 888–894.

Ren, H., and Wu, Y. (2011), Turbulent boundary layers over smooth and rough forward-facing steps, *Phys. Fluids*, Vol. 23(4), pp. 045102

Wu, Y., and Ren, H. (2013), On the impacts of coarse-scale models of realistic roughness on a forward-facing step turbulent flow, *Int. J. Heat Fluid Flow*, Vol. 40, pp. 15–31.

De Brederode, V., and Bradshaw, P. (1972), Three-dimensional flow in nominally two-dimensional separation bubbles: flow behind a rearward-facing step, Imp. Coll. Aeronaut. Rep., pp. 72–19.

Largeau, J. F., and Moriniere, V. (2006), Wall pressure fluctuations and topology in separated flows over a forward-facing Step." *Exp. Fluids*, Vol. 42, pp. 21–40.

Forliti, D. J., Strykowski, P. J., and Debatin, K. (2000), Bias and precision errors of digital particle image velocimetry, *Exp. Fluids*, Vol. 28(5), pp. 436–447.

Jovic, S. (1996), An experimental study of a separated/reattached flow behind a backward- facing step. Re (sub h) = 37, 000, *NASA Tech. Memor*, (110384).

Lu, S. S., and Willmarth, W. W. (1973), Measurement of the structure of the Reynolds stress in a turbulent boundary layer, *J. Fluid Mech.*, Vol. 60(part 3), pp. 481–511.